Th STZ1 03

Enhanced 3D Broadband Processing - A Case Study from the Edvard Grieg Field

N. Salaun* (CGG), V. Cavalie (CGG), P. Borisevitch (CGG), D. Hardouin (CGG) & A. Wright (CGG)

SUMMARY

Data acquired in shallow water environments often exhibit a strong acquisition pattern relating to variations in incidence angle, azimuth and source signature from inner to outer streamers. These variations must be accurately compensated for during processing to reveal a spatially consistent 3D image of the data. With modern broadband acquisition this problem becomes more challenging as the frequency spectrum is wider. This North Sea case study, acquired with a multi-level source and variable depth streamer, presents an enhanced processing sequence containing 3D processing steps using different parameters for each frequency range. Results show the advantage of such a sequence to achieve a high definition image from the very shallow to the deep reservoir target.

Introduction

Modern broadband towed streamer acquisitions aim to record frequencies from 2 to 200 Hz. The ability to recover this large frequency bandwidth with full 3D spatial consistency creates important processing challenges. Imaging is often impacted by residual multiple energy, noise coming from acquisition such as swell or interference noise, sparse sampling in the crossline direction, variation of azimuths, incidence angles and source signature between inner and outer cables. All these factors will generate acquisition patterns in seismic content between the different cables. These issues are particularly problematic in a shallow water context, and become significant at high frequencies. In this paper we demonstrate how high definition imaging can be achieved through the use of new sophisticated processing techniques on a North Sea dataset.

Case Study description

The Edvard Grieg field is located in the Utsira High area in the central North Sea. The reservoir is situated at a depth of approximately 1,900 meters, and consists of porous, fractured bedrock underlying a thin sandstone layer from the Lower Cretaceous age. Discovered in 2007, this field reached full production in 2015. During this period several seismic acquisitions were carried out in order to accurately image the reservoir. Situated below a thick chalk layer, its thin prograding sand layers are difficult to image. Under an average 100 meters water depth, the accurate imaging of shallow, dense, interlaced channels is also an important objective in understanding the recent geological activity of the region. With this goal in mind, a multi-level source and variable depth streamer survey was acquired in 2012 (Siliqi *et al.*, 2013). After delivery of a processed volume in 2014 with good imaging of the reservoir, the decision was made to reprocess this dataset using its latest possible technology in order to improve the 3D homogeneity and to obtain a higher resolution at the target.

Processing sequence

Four main processing steps of the enhanced sequence will be described and discussed in more detail: denoising, designature/deghosting, demultiple and post imaging signal enhancement.

In order to maximize the available bandwidth with good signal to noise ratio (S/N) a strong denoising sequence was applied. A combination of 3D erratic noise attenuation by joint low-rank and sparse inversion (Sternfels *et al.*, 2015) and 3D noise attenuation using sparse tau-p inversion (Ray *et al.*, 2015) enabled efficient denoising of both low and high frequencies while retaining coherency between cables.

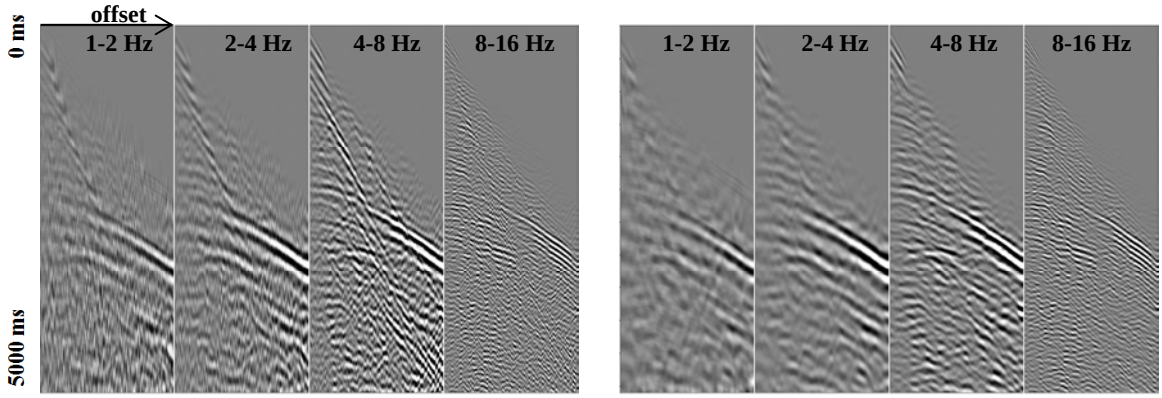

Figure 1 *Shot point, focused on low frequency panels, before (left) and after (right) combination of 3D erratic noise attenuation by joint low-rank and sparse inversion, 3D noise attenuation using sparse tau-p inversion and residual linear noise attenuation in tau-p domain.*

Multi-level source acquisition partially attenuates the source ghost by positioning airguns at more than one depth (Siliqi *et al*, 2013). The remaining residual source ghost may be corrected as part of

designature where a shaping filter that is designed to convert the farfield signature to a broadband spike is applied to the data (Poole *et al*, 2013). Usually vertical far-field designature is applied as a 1D filter even though the source response is not isotropic. To achieve more accurate broadband results for all angles, it is necessary to apply full directional designature where the source signal at all takeoff angles is corrected to the same broadband zero phase wavelet. Figures 2a-d compare data after 1D designature with 3D designature using notional sources derived from near-field hydrophone data (Ni *et al*., 2014). After stabilization of the wavelet, 3D receiver deghosting was applied to fully deghost shallow events on the outer cables. The approach was performed in the 3D progressive sparse tau-p domain taking into account all cables for one shot at the same time (Wang *et al*, 2014). Both low and high frequencies benefitted from the 3D application when compared to 2-D deghosting (Figure 2e-h).

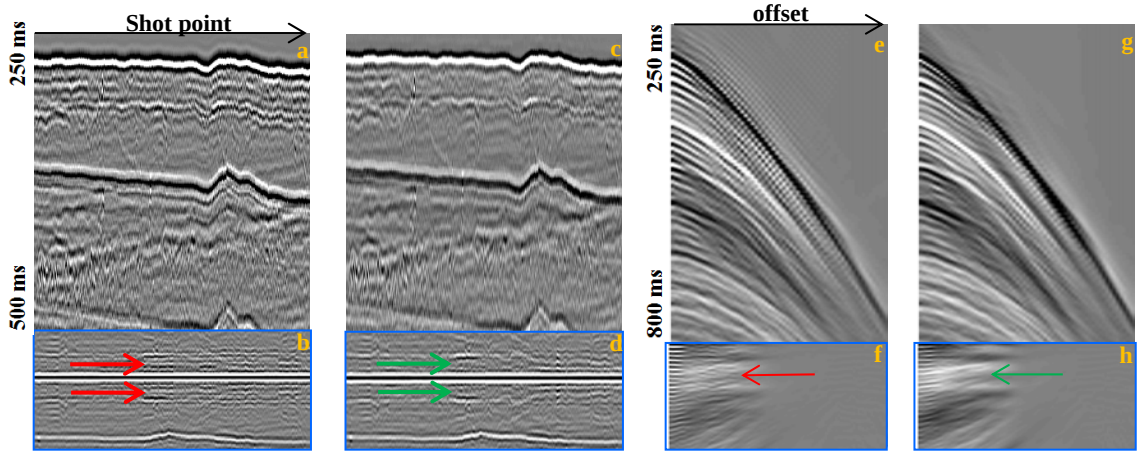

Figure 2 *Near receiver of outer cable: a) 1-D designature with autocorrelation (b), c) 3D designature with autocorrelation (d), Shot point of outer cable: e), 2-D deghosting with autocorrelation (f), g) 3D deghosting with its autocorrelation (h).*

Improvements in the spatial consistency of high frequencies with 3D designature and deghosting lead to enhanced resolution at the water bottom and of shallow complex channels. Good definition of these shallow events helps in building more accurate broadband multiple models.

In shallow water areas, water-layer primary reflections arrive at large propagation angles and as such are contaminated by other waves arriving at similar travel times, such as direct waves, head waves, and refracted waves. Demultiple sequences for these regions can typically include a combination of 3D-model-based water-layer demultiple (MWD) and muted SRME for longer period multiples. In order to achieve an effective demultiple result, a rigorous sequence was applied. 3D selective-input MWD (SIMWD) (Huang *et al*, 2015) was used to reduce the impact of missing near offsets for the multiple prediction on outer cables. For multiple energy generated by events located just below the water bottom, estimation of primaries by sparse inversion (EPSI) (Hu *et al*, 2015) was used. Use of EPSI avoided having to run several passes of MWD, the first pass for the water bottom and additional passes for slightly deeper events. EPSI also modeled events which were too shallow to be modeled by SRME. In addition, EPSI, with its iterative inversion process, managed to predict the full frequency multiple model with the correct phase and amplitude. A combination of SIMWD and EPSI models were then used for short period multiple attenuation. Global adaptation of a 3D SRME model completed the sequence for long period multiple attenuation. A least-squares adaptive subtraction was applied by splitting data and multiple models into octave ranges. This octave decomposition method allows adaptive filters to be designed and applied individually for each frequency range. A second pass of inversion-driven free surface multiple elimination (Poole *et al*, 2015), subtracted using 3D curvelet adaptive subtraction, removed remaining multiples below the chalk (Figure 3).

After migration, in order to fully recover the spectral bandwidth and to better control the wavelet, a time-variant amplitude and phase dispersion correction for broadband data (Yang *et al*, 2015) and a 3D conformal inversion (Peng *et al*, 2016) were applied (Figure 4).

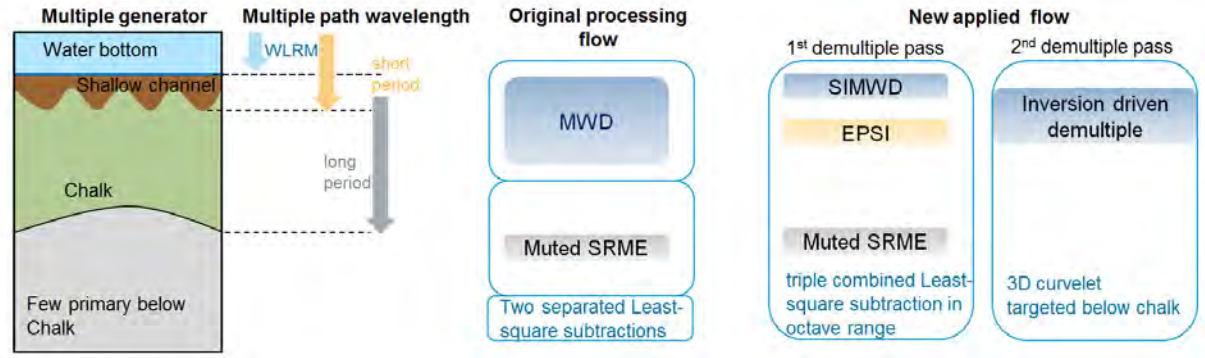

Figure 3 *Left: multiple generators classified by their depth. Middle: original shallow water de-multiple processing flow. Right: Proposed shallow water de-multiple flow.*

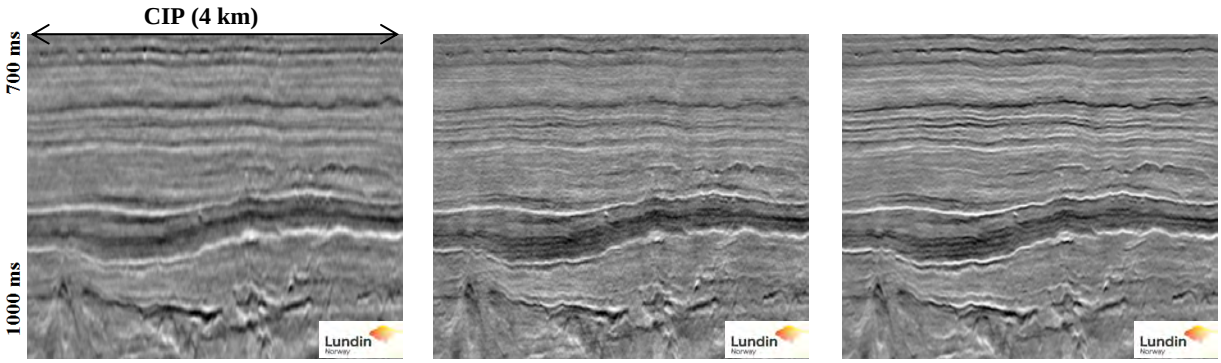

Figure 4 *PSDM section before (left), after broadband time-variant amplitude and phase dispersion correction (center) and after 3D conformal resolution enhancement (right).*

The processing sequence began with an effective de-noising flow which helped to recover a good S/N ratio even for very low frequencies; this brought valuable information on the final image (Figure 5a-b). This was followed by 3D designature and deghosting which fully took into account the source directivity and incidence angles, resulting in a consistent data quality for inner and outer cables even in this shallow water context. Complex shallow channels, interleaved with thin sediment layers, were subsequently imaged with very high resolution and the acquisition footprint was well attenuated (Figure 5c). At the reservoir level, a substantial demultiple sequence using various models for water layer related multiple, shallow period and long period multiples, all subtracted by octave ranges, revealed thin geological layers previously hidden by the strong multiple content. Thin events and diffractions were accurately preserved and fault planes sharply imaged (Figure 5d-e). Having a good S/N after the depth migration enabled the recovery of a wide spectrum. Clean low and high frequency information coupled with good phase control for all frequencies brought character to the section and greatly helped structural interpretation.

Conclusion

Accurate imaging in shallow water environments, especially at high frequencies, is heavily affected by strongly varying take-off angles from inner to outer streamers as well as coarse cable spacing and missing far cable near offsets. We have shown how the combination of broadband acquisition with an enhanced processing sequence containing 3D processing steps can result in a high definition image from the shallow section to the deep reservoir target. This robust sequence did not require any a priori information and can be applied to a variety of shallow water areas.

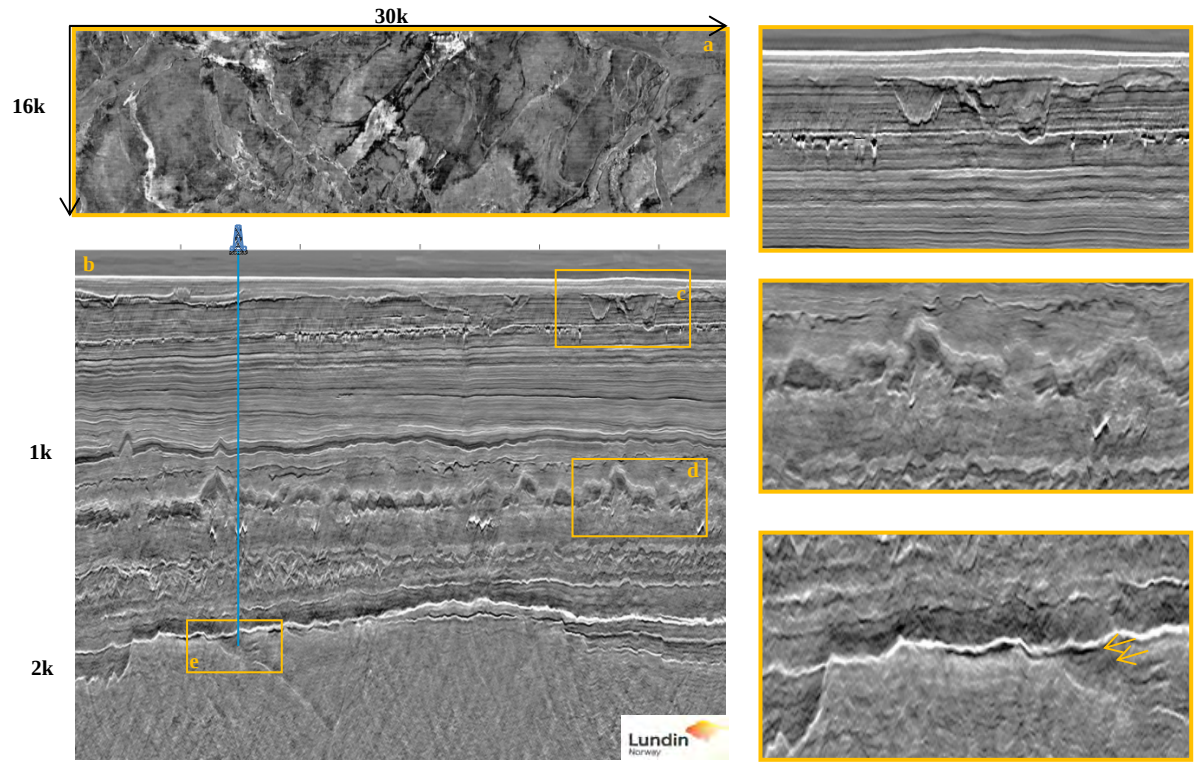

Figure 5 *Final migrated stack images. a) Time slice at 150 m depth showing complex interlaced channels, b) Inline section crossing Edvard Grieg well, zooms: c) shallow section showing channel and thin sediment layer, d) sticky shale zoom exhibiting complex low and high frequency events, e) Reservoir zoom showing thin sandstone layer (orange arrows) and complex faulting.*

Acknowledgements

We thank Lundin for permission to show these case study images and for their collaboration over the course of this project.

References

Hu, X., Qin, J., Liu, J. and Hembd, J. [2015] Estimation of Primaries by Sparse Inversion in Shallow Water - Practical Challenges and Strategies. *77th EAGE Conference and Exhibition 2015.*

Huang, H., Wang, P. and Hu, S. [2015] Selective-input Adaptation of Model-based Waterlayer Demultiple. *77th EAGE Conference and Exhibition 2015.*

Ni,Y., Payen, T. and Versin, A. [2014] Joint inversion of near-field and far-field hydrophone data for source signature estimation. *84rd Ann. Internat. Mtg*., SEG Expanded Abstracts, 57-61.

Peng, C., Bai, B., Liu, Y, and Fu, Z. [2016] *Structurally conformal resolution enhancement with joint sparse inversion.* Personal communication.

Poole, G., Davison, C., Deeds, J., Davies, K. and Hampson, G. [2013] Shot-to-shot directional designature using near-field hydrophone data. *83rd Ann. Internat. Mtg*., SEG Expanded Abstracts, 4236-4240.

Poole, G. and Cooper, J. [2015] Inversion-driven free surface multiple modelling using multi-order Green's functions. *85th Ann. Internat. Mtg*., SEG Expanded Abstracts, 4428-4432.

Ray, S., Z. Zhang, Z. Fu, L. Liu, and P. Wang. [2014] Noise attenuation using a dipole sparse Tau-P inversion. *84th Annual International Meeting, SEG*, Expanded Abstracts, 4213-4217.

Siliqi, R., Payen, T., Sablon, R. and Desrues, K. [2013] Synchronized multi-level source, a robust broadband marine solution. *83rd Ann. Internat. Mtg*., SEG Expanded Abstracts, 56-60.

Sternfels, R., Viguier, G., Gongoin, R. and Le Meur, D. [2015] Joint Low-rank and Sparse Inversion for Multidimensional Simultaneous Random/Erratic Noise Attenuation and Interpolation. *77th EAGE Conference and Exhibition 2015*.

Wang, P., Ray. and Nimsaila, K. [2014] 3D joint deghosting and Crossline interpolation for marine single-component streamer data. *84th Ann. Internat. Mtg*., SEG Expanded Abstracts, 3594-3598.

Yang, F., Sablon, R. and Soubaras, R. [2015] Time variant amplitude and phase dispersion correction for broadband data. *85th Ann. Internat. Mtg*., SEG Expanded Abstracts, 4620-4625.